# Magmatic-hydrothermal origin of granite-hosted Cu–Ba mineralization from southern Bundelkhand, Tikamgarh district, Madhya Pradesh, India

The Archaean to Palaeoproterozoic Bundelkhand Craton comprises older metamorphic rocks (metabasalt, metapelites, tonalite–trondhjemite–granodiorite gneisses and BIF), granitoids and late intrusive rocks into the granitoids, such as quartz reefs and mafic–ultramafic rocks[1]. Among these, granitoids cover >90% area in the craton, in which older metamorphic rocks are present as enclaves, while quartz reefs and basalt dikes intruded the granitoids. Sporadic occurrences of sulphide mineralization in Bundelkhand Granitoid Complex (BGC) have been reported which are mostly of Cu and Mo[2,3]. The presence of barite veins in the granitoids of Bundelkhand was first reported by Dubey[4]. These barite veins are 7 km southeast of Baldeogarh Town (Tehsil). These veins were again studied by Bagchi[5]. He reported quartz–barite veins mainly in three locations, namely Chakarda Hill, Durrenkheda and Bheronobar with presence of specks of chalcopyrite and malachite in the veins. However, the nature and origin of barite mineralization in such a vast granitic terrain has not been discussed so far.

A detailed field and petrographic study of the granitoids associated with the mineralized veins classified them into two varieties – hornblende granite (coarse-grained, equigranular to porphyritic and composed of K-feldspar, plagioclase, quartz, hornblende and biotite) and biotite granite (medium- to coarse-grained, non-porphyritic and composed of quartz, K-feldspar, plagioclase and biotite). The mineralized veins are found mainly at three locations: Bheronobar, Matiyaratar and Nayagaon (Figure 1). In Bheronobar, mineralized veins are mainly hosted by porphyritic hornblende granite while in Matiyaratar and Nayagaon, these veins are hosted by biotite granite. These mineralized veins are composed mainly of quartz and a varying proportion of barite with sulphide minerals mainly pyrite, chalcopyrite and covellite. Malachite stains are very common in these veins (Figure 2 *a*). The veins in the three localities have approximately similar dimensions, about 50 m long and 8 m thick. The vein near Bheronobar is N80°W–S80°E trending, whereas the other two veins are N20°W–S20°E trending. Barite was mainly colourless or white. Angular clasts of associated granite were found within these veins (Figure 2 *b*). Similar field characters of these veins suggest a common origin for them.

Petrographic studies were carried out to identify various sulphide mineral phases. Barite under a microscope is colourless, non-pleochroic, has moderate relief and shows first-order grey to pale yellow interference colour (Figure 2 *c*). Chalcopyrite, under reflected light, shows a golden yellow colour and is anhedral (Figure 2 *d*). Covellite development was observed at the margin of chalcopyrite grains (Figure 2 *e*). In addition, bornite was also identified by its characteristic honey-brown colour. To confirm the various sulphide mineral phases, EPMA analysis was carried out using an electron probe micro analyser (CAMECA SX 100)

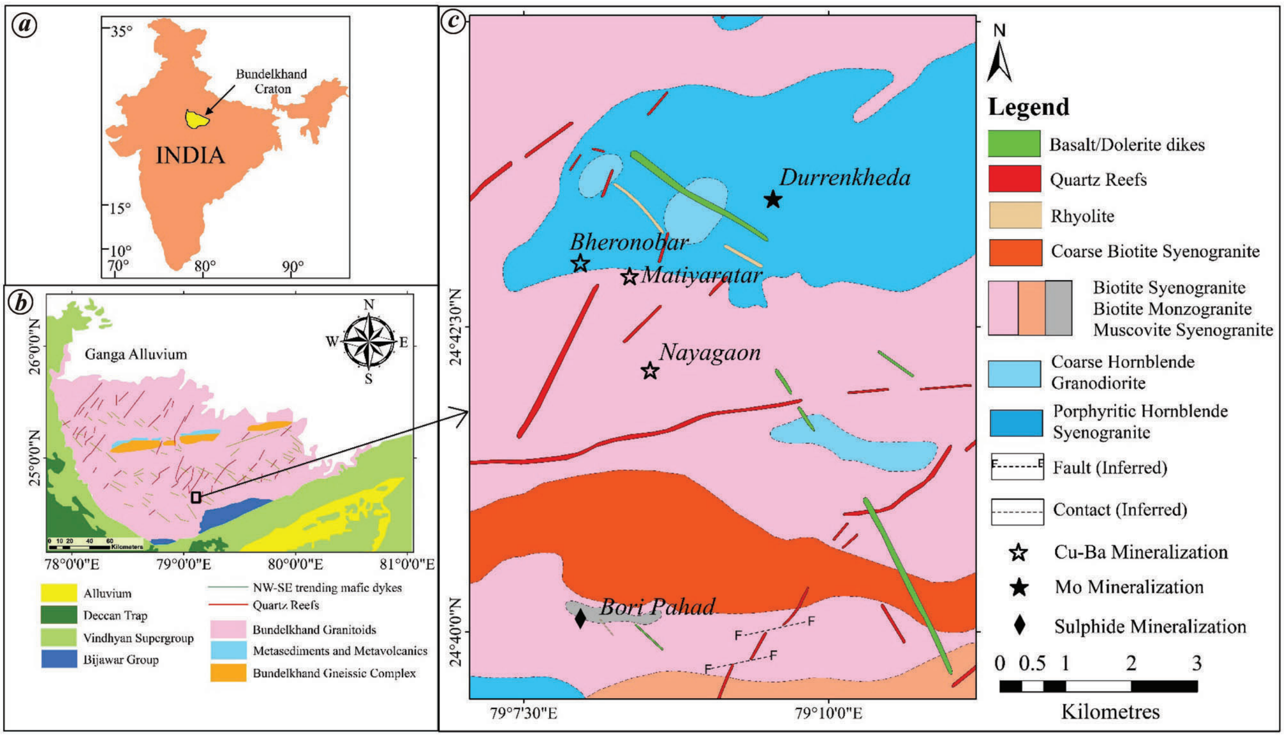


**Figure 1.** ***a***, Index map showing location of Bundelkhand craton in India. ***b***, Geological map of Bundelkhand Craton (after Basu[1]). ***c***, Geological map of the area around Bheronobar, Durrenkheda, Nayagaon and Dikoli areas showing various locations of mineralization.

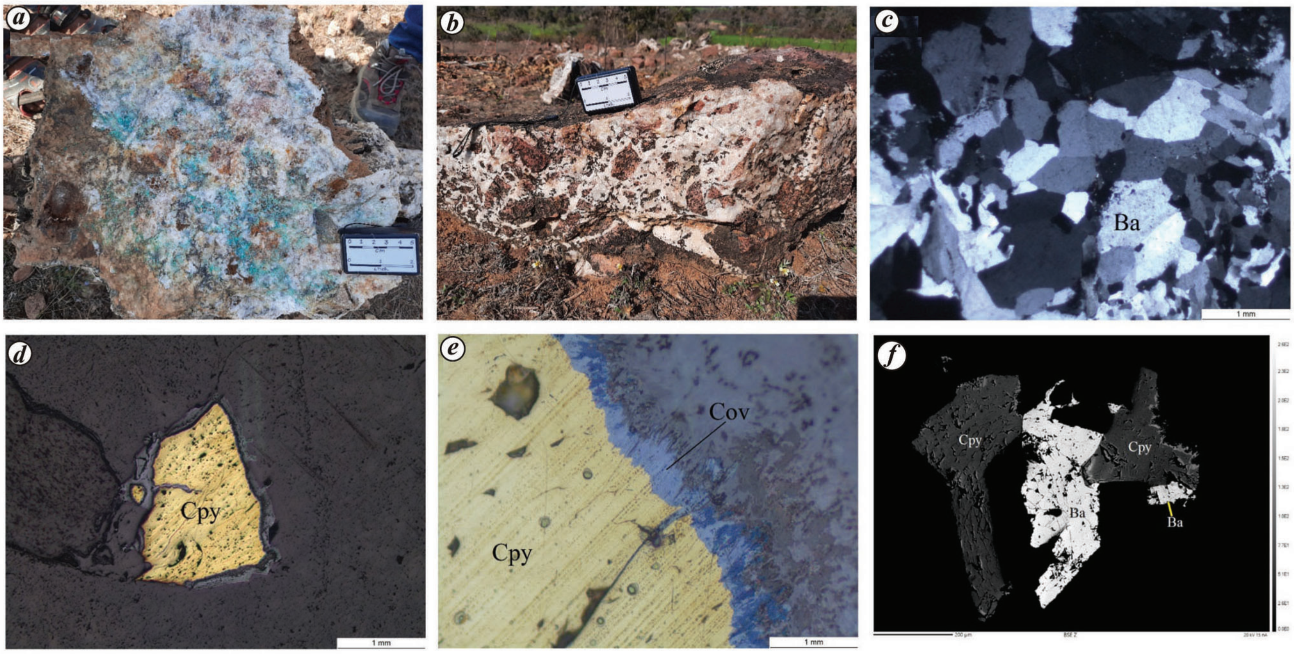


**Figure 2.** ***a***, A large chunk from the quartz–barite vein showing intense malachite staining; ***b***, Angular clasts of associated granite within the quartz–barite vein; ***c***, Barite under cross polar showing first order grey colour; ***d***, A chalcopyrite grain under reflected light; ***e***, Covellite at the margin of chalcopyrite; ***f***, BSE image showing association of barite and chalcopyrite. Ba, Barite; Cpy, Chalcopyrite; Cov, Covellite.

**Table 1.** EPMA data (in wt%) for barite and Cu bearing minerals form Quartz–Barite (Q–B) veins

Data for barite

| Sample | PS 147 | | | | | PS 235 | | |
|---|---|---|---|---|---|---|---|---|
| Data point | 4 | 7 | 11 | 15 | 16 | 21 | 22 | 23 |
| S | 12.48 | 12.24 | 13.05 | 12.36 | 13.18 | 12.95 | 12.98 | 12.65 |
| Cu | 0 | 0.33 | 0 | 0.14 | 0 | 0 | 0 | 0 |
| Fe | 0 | 0.63 | 0.02 | 0.2 | 0 | 0.09 | 1.03 | 0.15 |
| Co | 0 | 0 | 0.02 | 0 | 0 | 0 | 0 | 0 |
| Ni | 0.02 | 0 | 0 | 0 | 0 | 0 | 0 | 0 |
| Ba | 53.91 | 53.53 | 54.5 | 54.42 | 54.6 | 54.56 | 54.04 | 53.53 |

Data for Cu bearing phases

| Sample | PS 147 | | | | | | | | | | |
|---|---|---|---|---|---|---|---|---|---|---|---|
| Data point | 1 | 2 | s3 | 5 | 6 | 8 | 9 | 10 | 12 | 13 | 14 |
| S | 34.71 | 34.66 | 35.27 | 34.81 | 34.97 | 35.17 | 33.19 | 33.45 | 35.42 | 30.96 | 27.28 |
| Cu | 33.85 | 33.75 | 33.5 | 33.25 | 33.35 | 33.69 | 65.76 | 64.75 | 33.65 | 67.27 | 70.54 |
| Fe | 29.84 | 30.02 | 30.11 | 30.02 | 29.92 | 29.78 | 1.48 | 1.64 | 29.99 | 1.27 | 1.49 |
| Co | 0.01 | 0.03 | 0.04 | 0.06 | 0.04 | 0 | 0 | 0.02 | 0.02 | 0 | 0 |
| Ni | 0 | 0 | 0 | 0 | 0 | 0 | 0 | 0 | 0 | 0.01 | 0 |
| Ba | 0.1 | 0.07 | 0.06 | 0.09 | 0 | 0.08 | 0.13 | 0.15 | 0.11 | 0.28 | 0.25 |

| Sample | PS 235 | | | | | | | | | | |
|---|---|---|---|---|---|---|---|---|---|---|---|
| Data point | 17 | 18 | 19 | 20 | 24 | 25 | 26 | 27 | 28 | 29 | 30 |
| S | 35.42 | 1.77 | 34.69 | 1.11 | 35.04 | 34.58 | 33 | 33.47 | 35.01 | 34.97 | 35.63 |
| Cu | 33.73 | 17.93 | 33.85 | 17.18 | 33.89 | 35.24 | 63.03 | 62.72 | 33.86 | 34.13 | 33.91 |
| Fe | 29.7 | 34.74 | 30.24 | 34.92 | 30.13 | 28.91 | 1.89 | 2.31 | 29.98 | 29.99 | 29.94 |
| Co | 0.02 | 0.05 | 0.07 | 0.04 | 0 | 0.06 | 0.01 | 0 | 0.04 | 0.01 | 0 |
| Ni | 0 | 0 | 0 | 0 | 0 | 0 | 0 | 0 | 0 | 0 | 0.02 |
| Ba | 0.03 | 0.68 | 0.09 | 0.1 | 0.09 | 0.04 | 0.18 | 0.17 | 0.07 | 0.09 | 0.06 |

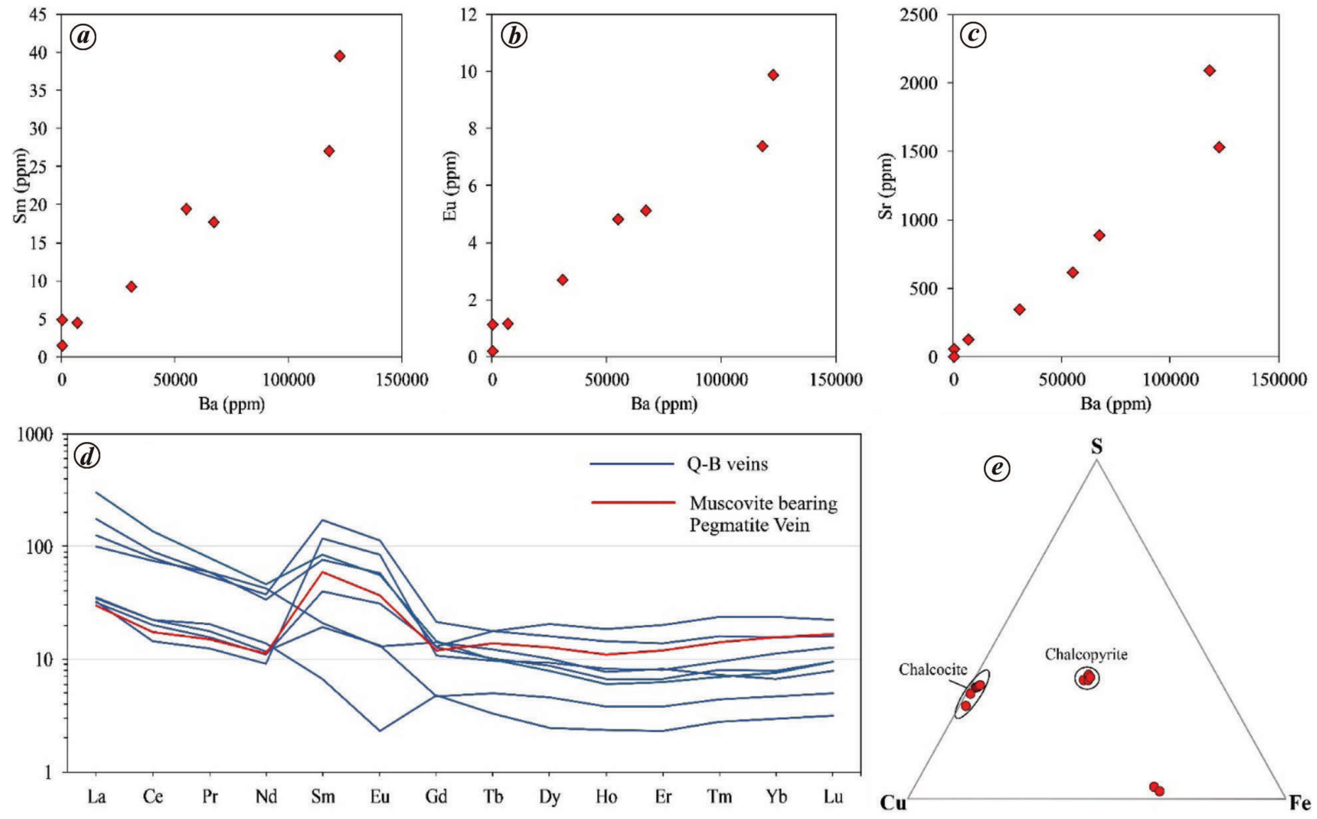


**Figure 3.** ***a***, Ba versus Sm plot; ***b***, Ba versus Eu plot; ***c***, Ba versus Sr plot; ***d***, REE patterns of the quartz barite veins; ***e***, S–Cu–Fe diagram for Cu bearing phases in quartz barite veins (after Mervin and Lombard[13]).

operating at an acceleration voltage of 20 kV, beam current of 15 nA and a beam size of 1 μm. Two selected samples were analysed, for which data is given in Table 1. The BSE images confirm the close association of chalcopyrite and baryte (Figure 2 *f* ).

Barite ($BaSO_4$) and Celestine ($SrSO_4$) form solid solution and may occur in a remarkably diverse range of sedimentary, metamorphic, and igneous environments[6]. In our samples, the Ba-bearing mineral phase showed a narrow range of high Ba between 53% and 54% (Table 1). Similarly, sulphur shows a narrow range between 12.25% and 13% indicating that barite is the only mineral phase. For Cu-bearing mineral phases, a plot is given in Figure 3 *e*, which shows three different groups in the data. The central group represents the chalcopyrite compositions with nearly equal Cu and Fe contents. The other group falling close to the Cu–S axis shows a composition between covellite and chalcocite. The third group falls close to Cu–Fe axis and shows a low concentration of sulphur and thus represents the altered chalcopyrite composition which possibly has gone through sulphur loss during alteration processes.

After confirming the presence of Cu–Ba mineral phases, eight vein samples were analysed at the chemical laboratory of the Geological Survey of India (GSI), Nagpur for selected trace and REE elements (Table 2). High values of Ba ranging from 3% to 12% were observed in the samples. Similarly, Cu values varied between 130 and 2275 ppm. The trace element data of mineralized veins showed that Ba had a high positive correlation with Sr, Eu and Sm (Figure 3 *a*, *b* and *d* respectively), which indicates that these elements had a strong affinity with Ba and therefore they possibly segregated along with Ba- and S-rich fluids from the same source.

Generally, barite deposits can be found in three forms: bedded sedimentary deposits, bedded volcanic deposits and vein or cavity-filling deposits[7]. The source of vein or cavity filling barite deposits may vary from sedimentary to igneous. In the study area, the Cu–Ba mineralization was mainly vein type. The barite-bearing veins were found in association with granite and there is no sedimentary rock in the vicinity of these veins. Therefore, field evidence indicates an igneous origin of the hydrothermal solutions that contributed to Cu–Ba mineralization. Although the mineralized veins in the area showed a complete igneous rock association, as mentioned above the barite can also form in VMS setting as well as a sedimentary bedded deposit, where hydrothermal solutions interact with sea-water. According to Mondal and Zainuddin[8], in southern Bundelkhand, an oceanic environment prevailed during the craton evolution. Therefore, the idea cannot be ignored that barite might have formed in an oceanic environment. Because of the highly identical nature of geochemical twins Y and Ho, these elements show near chondritic Y/Ho ratio (28) in most igneous rocks[9]. Any interaction with sea-water increases this ratio above the chondritic value[10]. In Cu–Ba-mineralized veins of the study area, this ratio ranges from 17 to 30.2 with three samples maintaining near chondritic values. This observation supports a magmatic origin for the Cu–Ba mineralization. In addition, all three mineralized veins in the area show very similar chondrite normalized REE pattern (Figure 3 *d*), indicating all these veins belong to similar origin. A pronounced Sm and Eu anomaly is a characteristic feature

**Table 2.** Trace and REE data (in ppm) for Q–B and pegmatite veins

| | | Rb | Y | Ba | Sr | Hf | Cu | La | Ce | Pr | Nd | Sm | Eu | Gd | Tb | Dy | Ho | Er | Tm | Yb | Lu | Y/Ho | Ce/La |
|---|---|---|---|---|---|---|---|---|---|---|---|---|---|---|---|---|---|---|---|---|---|---|---|
| BRS-11 | Q–B veins | 213 | 16.38 | 118,020 | 2094 | 3.95 | 1500 | 11.97 | 13.88 | 1.69 | 6.49 | 27.06 | 7.38 | 3.27 | 0.56 | 3.57 | 0.7 | 2.01 | 0.34 | 2.79 | 0.48 | 23.4 | 1.16 |
| BRS-14 | Q–B veins | 21 | 16.1 | 67,309 | 883 | 0.8 | 285 | 64.68 | 85.72 | 8.19 | 24.05 | 17.69 | 5.11 | 3.87 | 0.59 | 3.3 | 0.57 | 1.67 | 0.29 | 1.94 | 0.36 | 28.2 | 1.33 |
| BRS-15 | Q–B veins | 16 | 42.3 | 30,700 | 346 | 0.05 | 2250 | 11.72 | 19.23 | 2.16 | 7.81 | 9.28 | 2.69 | 3.94 | 1.04 | 7.87 | 1.57 | 5.03 | 0.85 | 5.86 | 0.84 | 26.9 | 1.64 |
| BRS-16 | Q–B veins | 10 | 8.84 | 6818 | 125 | 0.22 | 165 | 12.72 | 21.45 | 2.43 | 8.38 | 4.44 | 1.15 | 1.42 | 0.29 | 1.75 | 0.32 | 0.94 | 0.16 | 1.17 | 0.19 | 27.6 | 1.69 |
| BRS 24 | Q–B veins | 81 | 19.65 | 378 | 56 | 2.66 | n.d. | 36.94 | 71.32 | 8.14 | 30.44 | 4.89 | 1.14 | 4.36 | 0.71 | 3.82 | 0.65 | 2.06 | 0.26 | 1.67 | 0.3 | 30.2 | 1.93 |
| BRS-30 | Q–B veins | 32 | 34.53 | 122,602 | 1530 | 1.84 | 130 | 45.79 | 75.75 | 7.46 | 26.49 | 39.54 | 9.87 | 6.52 | 1.04 | 6.14 | 1.23 | 3.42 | 0.58 | 3.88 | 0.61 | 28.1 | 1.65 |
| BRS-31 | Q–B veins | 19 | 13.26 | 55,164 | 616 | 1.13 | 390 | 111.6 | 131 | 10.82 | 32.74 | 19.44 | 4.82 | 4.42 | 0.57 | 3.01 | 0.51 | 1.55 | 0.25 | 1.86 | 0.36 | 26.0 | 1.17 |
| BRS-40 | Q–B veins | 22 | 3.56 | 84 | n.d. | 1.42 | 2275 | 13.01 | 21.43 | 2.83 | 9.76 | 1.54 | 0.2 | 1.45 | 0.19 | 0.93 | 0.2 | 0.58 | 0.1 | 0.73 | 0.12 | 17.8 | 1.65 |
| BRS-37 | Pegmatite veins | 285 | 17.76 | 35,845 | 444 | 5.59 | 405 | 10.91 | 16.78 | 2.07 | 7.93 | 13.76 | 3.18 | 3.66 | 0.8 | 4.85 | 0.93 | 3 | 0.51 | 3.88 | 0.64 | 19.1 | 1.54 |

of these veins and there is no significant enrichment of LREE or HREE. Barium segregation from a system can also lead to segregation of Eu and Sm[11]; therefore, the positive correlation of Sm and Eu with Ba clearly explains these anomalies in the REE pattern. Interestingly, one sample of muscovite-bearing pegmatite vein showed a similar REE pattern and 3.5% Ba. This suggests a similar source for the quartz-barite veins and muscovite-bearing pegmatite veins in this part of the Bundelkhand craton.

The field characteristics of the Cu–Ba mineralization in the area do not show any sedimentary structure, rather, it is vein type. The presence of angular clasts of host granite in these veins indicate that the mineralizing fluids were possibly channelled through faults or fractures within the granites. Such field characters indicate a hydrothermal origin of the Cu–Ba mineralization. The trace element characters of the mineralized veins show a high Ce/La ratio (1.16 to 1.93). Marine barites have a low Ce/La ratio (Ce/La = 0.33) while terrestrial barites show a high Ce/La ratio (Ce/La = 1.37)[12]. Thus, the high Ce/La ratio in our samples clearly shows that mineralizing fluids were not of any marine origin, therefore, a sedimentary source for the Cu–Ba mineralization cannot be asserted. Similarly, as mentioned above, these veins show near chondritic Y/Ho ratio in our samples, suggesting that mineralizing fluids had no interaction with sea-water. Thus, field and trace element characteristics of Cu–Ba mineralization lead us to an important outcome, that the Cu–Ba mineralization in the study area is of hydrothermal origin where the mineralizing fluids were not of marine origin nor they interacted with the marine water. Additionally, there is no sedimentary or metamorphic lithounit regionally, which could source barium. In that case, granites associated with the Cu–Ba mineralized veins, become the prime candidate to be the source of Cu–Ba mineralization. This is also supported by high Ba in muscovite-bearing pegmatite veins, which also shows a similar REE pattern. Therefore, we suggest that hydrothermal fluids, which gave rise to the Cu–Ba mineralization in the study area, were of magmatic origin. Since these veins intruded both porphyritic hornblende granite as well as biotite granite, it is difficult to assert which granite can be the actual source and, therefore, detailed studies can be carried out in this regard. Therefore, based on the field and geochemical characteristics of these mineralized veins, it can be said that the Cu–Ba mineralization in Durrenkheda, Bheronobar and Matiyara areas are of magmatic-hydrothermal origin. Petrographic studies confirm the association of Cu and Ba in these veins. Although, it must be mentioned that at all these locations, the excavated trenches are not deeper than 5 m indicating that no attempt has been made to find the sub-surface deposit, if any. Therefore, it is evident that geophysical studies are very much crucial for future exploration of Cu–Ba mineralization from the southern part of Bundelkhand.


1. Basu, A. K., *Rec. Geol. Surv. India*, 1986, **117**(II), 61–124.
2. Pati, J. K., Panigrahi, M. K. and Chakraborty, M., *J. Earth Syst. Sci.*, 2014, **123**, 943–958.
3. Gautam, N. and Deepu, T. R., *Rep. Geol. Surv. India*, 2016, Item No. 008/STM/CR/MP/2015/006.
4. Dubey, V. S., *Trans. Indian Ceram. Soc.*, 1942, **1**, 108–111; doi:10.1080/0371750X.1942.11011943.
5. Bagchi, T. C., *Rep. Geol. Surv. India*, 1951. Accession No. CHQ-12338.
6. Hanor, J., *Rev. Mineral. Geochem.*, 2000, **40**, 193–275; doi:10.2138/rmg.2000.40.4.
7. Johnson, C. A., Piatak, N. M. and Miller, M. M., *US Geol. Surv. Prof. Pap.*, 2017; doi:10.3133/pp1802D.
8. Mondal, M. E. A. and Zainuddin, M., *Terra Nova*, 1996, **8**, 532–539.
9. Bau, M., *Contrib. Mineral. Petrol.*, 1996, **123**, 323–333.
10. Zhao, K. D. and Jiang, S. Y., *Geochem. J.*, 2007, **41**, 121–134.
11. Chang, C., Qu Fu and Wang, X., *Geofluids*, 2019; doi:10.1155/2019/9797326.
12. Church, T. M. and Bernat, M., *Earth Planet. Sci. Lett.*, 1972, **14**(1), 139–144.
13. Mervin, H. E. and Lombard, R. H., *Econ. Geol.*, 1937, **32**, 203–284.



ACKNOWLEDGEMENTS. This work was carried out as field survey programme (M1AGCS-STM/NC/CR/SU-MP-JBP/2019/29665) of GSI. We are highly thankful to Ministry of Mines for funding of the project. We are grateful to V. P. Gaur (GSI, Bhopal) for his suggestions. We also express our gratitude to Shri Tapan Pal (DDG retired) and Shri S. Sarkar (DDG, SU: Madhya Pradesh, Jabalpur) for logistics and administrative support.

Received 5 July 2022; revised accepted 31 October 2022



ABHINAV KUMAR*
GEETA BIND
DIPAK HAZRA

*Geological Survey of India,*
*Sanjivani Nagar,*
*Jabalpur 482 003, India*
**For correspondence.*
*e-mail: kkabhinavkk@gmail.com*